



# The effect of clay treatment on remediation of diethylketone contaminated wastewater: Uptake, equilibrium and kinetic studies

Cristina Quintelas\*, Hugo Figueiredo, Teresa Tavares

IBB-Institute for Biotechnology and Bioengineering, Centre of Biological Engineering, University of Minho, Campus de Gualtar 4710-057, Braga, Portugal

## ARTICLE INFO

### Article history:

Received 11 March 2010  
Received in revised form  
17 November 2010  
Accepted 30 November 2010  
Available online 8 December 2010

### Keywords:

Adsorption  
Clays  
Solvent  
Ketones

## ABSTRACT

The ability of four different clays to adsorb diethylketone was investigated in batch experiments aiming to treat wastewater with low solvent concentrations. The adsorption performance in terms of uptake followed the sequence: vermiculite > sepiolite = kaolinite = bentonite, for all the adsorbent doses tested (from 0.1 to 1.5 g) in 150 mL of ketone solution (800 mg/L). The equilibrium data in the batch systems were described by Sips and Dubinin–Raduskevich isotherms. The best fits for bentonite and kaolinite clays were obtained with the Sips isotherm and for sepiolite and vermiculite the best fits were obtained with the Dubinin–Raduskevich model. Kinetic data were described by pseudo-first and pseudo-second order kinetics models. The best fit was obtained for the pseudo-first order model which assumed that the interaction rate was limited only by one process or mechanism on a single class of sorbing sites and that all sites were time dependent. The presence of functional groups on the clay surface that might have interacted with the solvent was confirmed by FTIR. XRD analysis was also performed. This study showed that the tested clays are very effective for the removal of diethylketone from industrial effluents.

© 2010 Elsevier B.V. All rights reserved.

## 1. Introduction

The problem of solvents in industrial effluents is well known. These substances are subject to severe restrictions on the levels in the environment because of their direct danger to health and natural ecosystems. Ketones are employed commonly in numerous industries (e.g. chemical, electronic, pharmaceutical) where they may act as a substrate or as a solvent in the production of drugs, vitamins and cosmetics [1]. Diethylketone is used as a solvent and as an intermediate in the synthesis of pharmaceuticals, flavors and pesticides.

The traditional technologies used for the treatment of chlorinated and ketone solvents are adsorption on granular activated carbon (GAC) and air-stripping. However, some efforts have been made on the use of biosorbents for the treatment of wastewaters contaminated with solvents. Pielech-Przybylska et al. [1] used a trickle-bed biofilter for the degradation of acetone. Osuna et al. [2] investigated the degradation of dichloromethane using two up-flow fixed-bed reactors inoculated with activated sludge and GAC as a support. Wu et al. [3] used *Bacillus circulans* for the degradation of the same solvent. Tsai et al. [4] and Wang and Tseng [5] studied the removal of trichloroethylene by oxidation and biodegradation, using a combination of iron particles and of autotrophic hydrogen-bacteria, respectively.

GAC is prohibitively expensive for industrial scale, air-stripping and biofilters from operational and equipment perspectives. Microorganisms are too sensitive to the xenobiotic effect of high concentrations of solvent. Also, they require nutrients and operational conditions (sterilization, eventual leaching prevention, etc.) that are difficult to obtain and maintain in an industrial environment.

Natural adsorbents such as clays and zeolites have been studied due to availability, low cost, simplicity of extraction and retention capacity. Clays have been used with success for the treatment of wastewaters contaminated with metals [6]. The large surface area of natural clay particles, the chemical and mechanical stability and the high cation-exchange capacity account for the excellent capacity of the clay to adsorb heavy metals [7,8]. Special attention has been given to vermiculite clay as adsorbent for copper and chromium ions [8], bentonite clay for the removal of a cationic dye [9], kaolin clay to remove Cd(II), Cr(VI), Fe(III) and Ni(II) [10], sepiolite clay as adsorbent of Cd(II), Cr(III) and Mn(II) [11] and as adsorbent of dyes [12].

This work aims the development of an environmental-friendly technology applicable to the treatment of aqueous solutions contaminated with low concentrations of solvents. Due to its widespread use, special attention will be given to the solvent diethylketone. Batch assays were performed aiming to investigate the adsorption behaviour of four different clays on the treatment of diethylketone aqueous solutions. The effect of the mass of adsorbent was studied. Experimental equilibrium results were analysed using the Dubinin–Raduskevich and Sips adsorption isotherms

\* Corresponding author. Tel.: +351 253604400; fax: +351 253678986.  
E-mail address: [cquintelas@deb.uminho.pt](mailto:cquintelas@deb.uminho.pt) (C. Quintelas).

and kinetic data were analysed by pseudo-first and pseudo-second order models. The presence of functional groups that may have a role in the adsorption process was evaluated by FTIR analyses of the clays. Phase analysis was also performed by XRD.

## 2. Materials and methods

### 2.1. Materials

Aqueous diethylketone solutions were prepared by diluting diethylketone (98%, acros organics) in distilled water. The kaolinite was obtained from Minas de Barqueiros, S.A. (Apúlia, Portugal) (average diameter of 2.37  $\mu\text{m}$ , BET surface area of 13.7  $\text{m}^2/\text{g}$ , porosity of 45.5%), sepiolite was obtained from Tolsa, S.A. (Spain) (average diameter of 0.58  $\mu\text{m}$ , BET surface area of 108  $\text{m}^2/\text{g}$ , porosity of 49%), bentonite clay was collected in Alentejo (Portugal) (average diameter of 0.2  $\mu\text{m}$ , BET surface area of 11.9  $\text{m}^2/\text{g}$ , porosity of 11%) and vermiculite was obtained from Sigma–Aldrich (average diameter of 0.45  $\mu\text{m}$ , BET surface area of 39  $\text{m}^2/\text{g}$ , porosity of 10%). All the experimental work was done in duplicate.

### 2.2. Methods

#### 2.2.1. Batch adsorption assays—uptake and equilibrium studies

The adsorption isotherms for the ketone by the four different clays were obtained from batch experiments at 25 °C. The experiments were performed in 250 mL Erlenmeyer flasks containing 150 mL of the ketone solution and different amounts of clay (0.1 g, 0.25 g, 0.5 g, 0.75 g, 1 g and 1.5 g). The initial concentration of the ketone solution was 800 mg/L. The flasks were rotated at a constant rate of 150 rpm until equilibrium was reached. Previous assays were made to determine the time needed for attaining equilibrium (13 days). Samples of 5 mL were taken after equilibrium was reached, centrifuged at 2500  $\times$  g for 5 min and the supernatant liquid was analysed for the ketone using GC (Chrompack CP 9001) equipped with a flame ionization detector (FID).

#### 2.2.2. Batch adsorption assays—kinetics study

The adsorption kinetics study was carried out using 250 mL Erlenmeyer flasks with 0.1, 0.25, 0.5, 0.75, 1 and 1.5 g of each clay and 150 mL of 800 mg/L of ketone solution. The assays were conducted in duplicate for all clays in an orbital shaker at 150 rpm for a period of 14 days at room temperature (25 °C). From the duplicate flasks, 0.3 mL samples were collected at established time intervals. The samples were analysed using GC (Chrompack CP 9001) with FID (flame ionization detector).

#### 2.2.3. Characterization procedures

Infrared spectra of the clays were obtained using a Fourier transform infrared spectrometer (FTIR BOMEM MB 104). Clays were centrifuged, dried and weighted. Finely ground clays (10 mg) were encapsulated in 100 mg of KBr in order to prepare translucent sample disks.

Phase analysis was performed by XRD using a Philips PW1710 diffractometer. Scans were taken at room temperature in a  $2\theta$  range between 5 and 60 °C, using Cu K $\alpha$  radiation.

The GC employed herein was a Chrompack CP 9001, equipped with a flame ionization detector (FID), and separations were performed using a TRB–Wax capillary column (30 m  $\times$  0.32 mm i.d.  $\times$  0.25  $\mu\text{m}$ ). The operating conditions were as follows: the column was held initially at a temperature of 50 °C, then raised at 10 °C/min to 100 °C, held at 100 °C for 4 min, then raised again at 40 °C/min to 200 °C and finally held at 200 °C for 2 min. The temperature of injector and detector were maintained at 250 °C. Nitrogen was used as a carrier gas at a flow rate of 30 mL/min and the injec-

tions were made in the split mode with a split ratio of 1:14. Under these conditions, the retention time for ketone was 2.2 min.

## 3. Results and discussion

### 3.1. FTIR and XRD analyses

The FTIR spectra of the clays, in the range of 500–4000  $\text{cm}^{-1}$  were taken to confirm the presence of functional groups that might be responsible for the adsorption process and presented in Fig. 1. As may be seen, clays display a number of absorption peaks, reflecting the complex nature of the clays. For kaolinite clay the main bands observed are the –OH stretching, hydroxyl sheet at 3695 and 3620  $\text{cm}^{-1}$ , the SiO stretching at 1062 and 1030  $\text{cm}^{-1}$ , the OH deformation at 912  $\text{cm}^{-1}$  and the mixed SiO deformations and octahedral sheet vibrations at 790, 753 and 694  $\text{cm}^{-1}$  [13]. For bentonite, bands were observed for the signals at 3425 and 3620  $\text{cm}^{-1}$ , which are due to stretching bands of the OH groups, 1635  $\text{cm}^{-1}$  which is assigned to the OH deformation, 1032  $\text{cm}^{-1}$  assigned to the Si–O vibrations within the layer and the band at 521  $\text{cm}^{-1}$  from the Si–O–Al, where Al is an octahedral cation [14]. The spectrum of sepiolite present a band at 3560  $\text{cm}^{-1}$  that is ascribed to the OH stretching vibration in the external surface of sepiolite and a band at 1655  $\text{cm}^{-1}$  that is assigned to the OH stretching, representing the bound water coordinated to magnesium in the octahedral sheet. The band at 1421  $\text{cm}^{-1}$  is due to the hydroxyl bending vibration which again reflects the presence of bound water [15]. According to the same author, the band at 1022  $\text{cm}^{-1}$  represents the stretching of Si–O in the Si–O–Si groups of the tetrahedral sheet. As for bentonite, the bands at 783 and 692  $\text{cm}^{-1}$  represent the mixed SiO deformations and octahedral sheet vibrations. For vermiculite, the band at 3400  $\text{cm}^{-1}$  represents the OH functional group stretching vibration [16]. The band at 1635  $\text{cm}^{-1}$  is for H–O–H in absorbed water bending and at 997  $\text{cm}^{-1}$  is for the Si–O–Si stretching [17]. Some of these band signals were also found by several other authors on clays corresponding to surface groups responsible for the adsorption of hazardous materials [14,15] and hence these groups may interact with the solvents in the present case.

The powder XRD diffraction patterns of the original clays and of the clays after contact with diethylketone were recorded at  $2\theta$  range between 5 and 60 °C and some representative patterns are presented in Fig. 2. All samples exhibited the typical and similar pattern of clays, with no obvious change in the position or in the relative intensity of the diffraction lines for clays after contact with diethylketone. The similarity between the diffractograms reveals that these processes do not promote any structural modification in the clays.

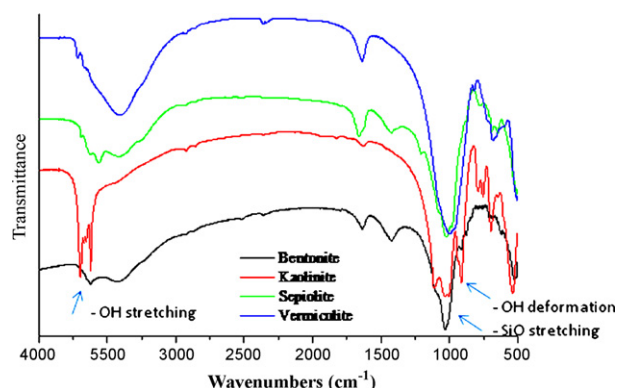


Fig. 1. FTIR spectra of the clays bentonite, sepiolite, kaolinite and vermiculite.

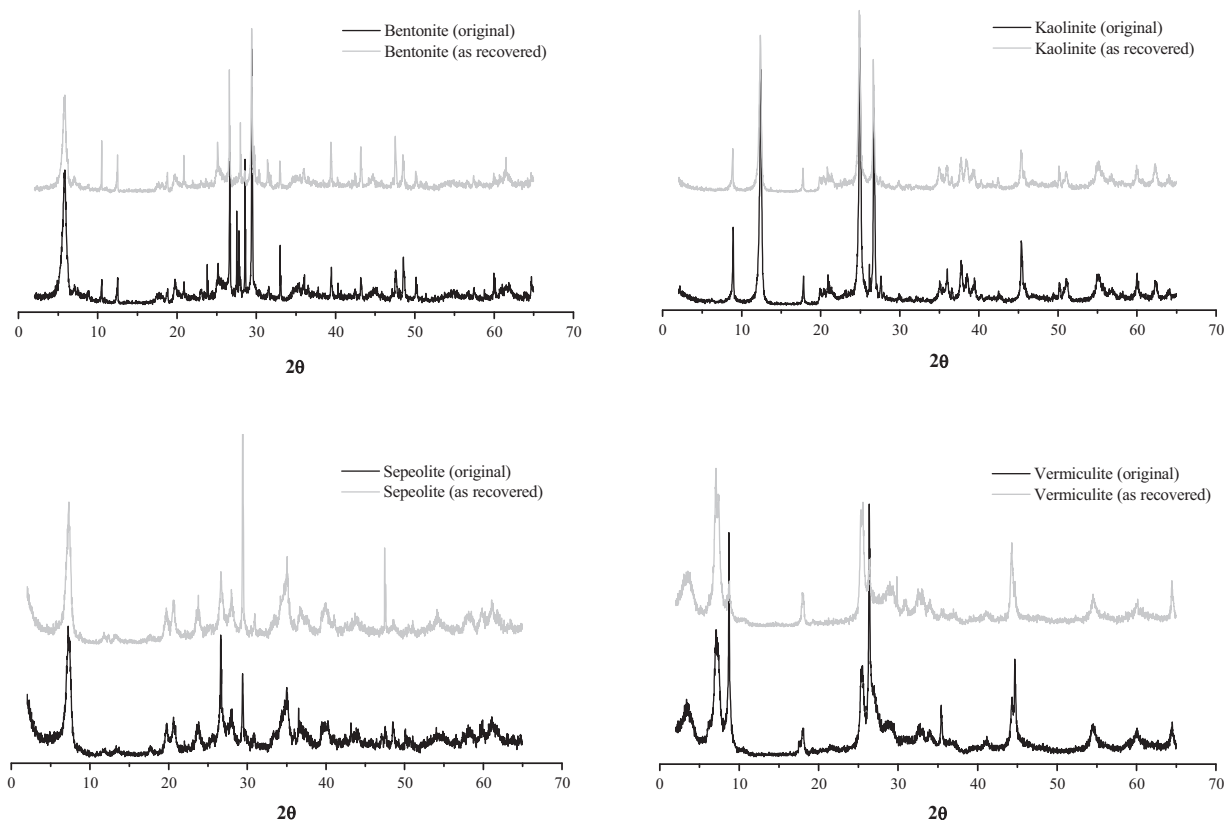


Fig. 2. XRD patterns of original and recovered clays.

### 3.2. Adsorption assays

#### 3.2.1. Batch adsorption assays—uptake studies

The experimental assays were made using a solution of solvent with initial concentration of 800 mg/L and masses of clay between 0.1 and 1.5 g. The removal of diethylketone by the different clays showed similar profiles for the range of adsorbent doses used. For example, Fig. 3 demonstrates the removal ratios of the solvent for the adsorbent doses of 0.1 and 1 g. The removal of solvent by the clays presented a typical and well known adsorption kinetics, quite rapid initially, but it gradually becomes slower with time. The initial higher rate may be due to the starting availability of the uncovered surface area of the adsorbent, since adsorption kinetics depends on the surface area of the adsorbent. The results showed that the solvent was almost completely removed by both systems, due to the affinity between the organic molecules and the clays [18].

Batch adsorption data showed slight differences in the performance between the four clays. The clays used are typical clays: kaolinite has a 1:1 layer (1:1 dioctahedral phyllosilicate) and sepiolite, bentonite and vermiculite consist of tetrahedral–octahedral–tetrahedral sheets (2:1 layer). On the last three clays, the two tetrahedral silicate layers are bonded together by one octahedral magnesium hydroxide-like layer and the structure is often referred to as 2:1 phyllosilicate. When tetravalent silicon is substituted by trivalent aluminum in the tetrahedral layer of the clay sheet, a negative charge is generated on the layer and, thus, hydrated magnesium is adsorbed on the tetrahedral layer between the sheets to maintain electro neutrality [8]. Usually, formation of organophilic clays after reaction with amines takes place via intercalation in the interlayer. These characteristics of clays make them a powerful sorbent for neutral organic molecules and organic cations [18]. The sequence in terms of uptake values is vermiculite > sepiolite = kaolinite = bentonite, for all the adsorbent

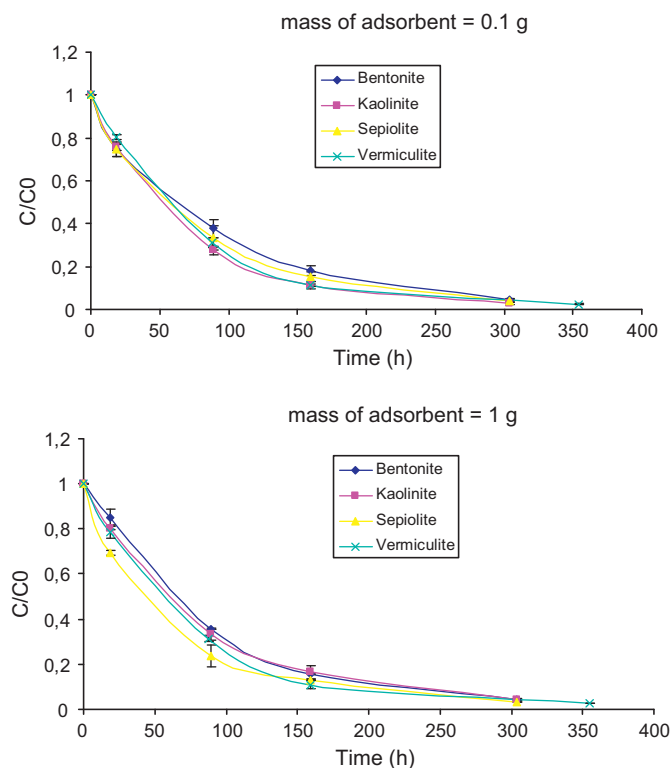


Fig. 3. Ratio between residual and initial solvent concentration ( $C/C_0$ ) as a function of contact time, for adsorbent doses of 0.1 and 1 g.

**Table 1**  
Adsorption isotherm constants for the best fit models, for the solvent onto bentonite, sepiolite, kaolinite and vermiculite clays.

Bentonite				
Best fit model	$K_s$	$a_s$	$b_s$	$R^2$
Sips	0.055	-2.269	0.253	0.96
Kaolinite				
Best fit model	$K_s$	$a_s$	$b_s$	$R^2$
Sips	0.007	-0.226	-0.385	0.93
Sepiolite				
Best fit model	$q_D$	$B_D$	$R^2$	
Dubinin–Radushkevich	0.620	0.0002	0.70	
Vermiculite				
Best fit model	$q_D$	$B_D$	$R^2$	
Dubinin–Radushkevich	0.684	0.0002	0.69	

doses tested. In terms of removal percentage, the results were better for vermiculite clay with values greater than 97%. Several authors verified an increase in the removal percentage when the adsorbent dose was increased [19,20], as a result of increased surface area and increased adsorption site availability due to increased adsorbent dose. This trend was not verified in the present study where the removal percentages remain around 96–97% for all the adsorbent doses used.

### 3.2.2. Modelling of equilibrium studies

Through the modelling of equilibrium data it is possible to characterize adsorbents under various operational conditions and to describe how adsorbates interact with the adsorbents. The equilibrium experiments were performed by varying the mass of adsorbent between 0.1 and 1.5 g for an initial solvent concentration of 800 mg/L, in 150 mL of solution. The time for the equilibrium to be reached was previously determined.

Two different isotherm equations were used to fit the experimental equilibrium adsorption data. Sips [21] proposed an equation that can be expressed by:

$$Q_e = \frac{K_s C_e^{1/b_s}}{1 + a_s C_e^{1/b_s}} \quad (1)$$

$K_s$  ( $L^{b_s} \text{ mg}^{1-b_s}/\text{g}$ ),  $a_s$  ( $L/\text{mg}$ ) $^{b_s}$  and  $b_s$  are the Sips isotherm parameters. This equation is also called Langmuir–Freundlich isotherm and the name derives from the limiting behaviour of the equation. At low sorbate concentrations it effectively reduces to a Freundlich isotherm and thus does not obey Henry's law. At high sorbate concentrations, it predicts the monolayer sorption capacity characteristics of the Langmuir isotherm.

Dubinin and Radushkevich [22] have reported that the characteristic sorption curve is related to the porous structure of the sorbent. The Dubinin–Radushkevich equation is generally expressed as follows:

$$Q_e = q_D \exp \left( -B_D \left[ RT \ln \left( 1 + \frac{1}{C_e} \right) \right]^2 \right) \quad (2)$$

The constant,  $B_D$ , is related to the mean free energy of sorption per gram of the sorbate as it is transferred to the surface of the solid from infinite distance in the solution.  $T$  is the temperature (K) and  $R$  is the universal gas constant.

The constants calculated for the best fit are presented in Table 1. As an example, the comparison between the experimental results and those predicted by the best fit model, for bentonite clay, is shown in Fig. 4. For bentonite and kaolinite the best fit model was

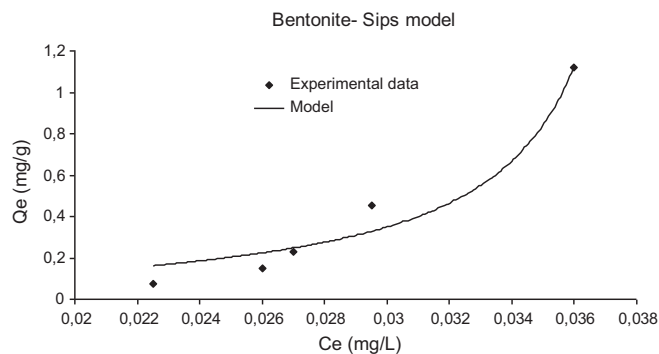


**Fig. 4.** Best fit sorption isotherm for diethylketone onto bentonite clay (•: experimental data, —: model).

the Sips model. On the other hand, for the sepiolite and vermiculite clays the best fit was obtained by the Dubinin–Radushkevich model although the correlation coefficient was only approximately 0.7 which means that the models tested do not fit properly the isotherm obtained.

### 3.2.3. Modelling of kinetic data

The sorption kinetics is very important for the process design and operation control of an adsorption process. In wastewater treatment such kinetics are significant as they provide valuable insights into the reaction pathways and mechanism of sorption reactions. This allows the description of the solute uptake which in turn controls the residence time of sorbate at the solid–solution interface [23]. The kinetic experiments were performed by varying the mass of adsorbent between 0.1 and 1.5 g for an initial solvent concentration of 800 mg/L, in 150 mL.

As it was said before, the adsorption kinetics exhibited an immediate rapid adsorption and reached pseudo adsorption equilibrium within a short period of time (Fig. 2). The initial adsorption of solvent is a surface phenomenon, probably with diethylketone molecules replacing water molecules on the surface of clays. In the first stage the vacant sites in clay particles were saturated up rapidly at the initial stages and followed a linear progression. In the second stage there was a slow migration and diffusion of the compound (the rate of adsorption decreased and reached steady state) into the mineral structure [24]. Tahir and Raulf [9] explained the mechanism of adsorption on clays by a three step mechanism: first, the adsorbate species migrate from the bulk liquid phase to the outer surface of adsorbent particles (film diffusion); secondly, the solvent species move within the micro and macro-pores of adsorbent particles (pore diffusion) and at the end, the interaction between the adsorbate and the adsorbent species takes place within the surface.

The experimental adsorption kinetic data were modelled using pseudo-first and pseudo-second order equations. The linearized form of the pseudo-first order model [25] and pseudo-second order model [26] are shown below as Eqs. (3) and (4), respectively:

$$\log(q_e - q_t) = \log(q_e) - k_1 \cdot t \quad (3)$$

$$\frac{t}{q_t} = \frac{1}{(k_2 \cdot q_e^2) + t/q_e} \quad (4)$$

where  $q_e$  is the amount of solvent sorbed at equilibrium (mg/g),  $q_t$  the amount of solvent sorbed at time  $t$  (mg/g),  $k_1$  the pseudo-first order rate constant ( $\text{h}^{-1}$ ) and  $k_2$  is the pseudo-second order rate constant ( $\text{g}/\text{mg h}$ ). The rate constants predicted equilibrium uptakes and corresponding correlation coefficients for all the adsorbent doses tested have been calculated. They are summarized in Table 2. The plots of both, first and second order models, are shown in Figs. 5 and 6.

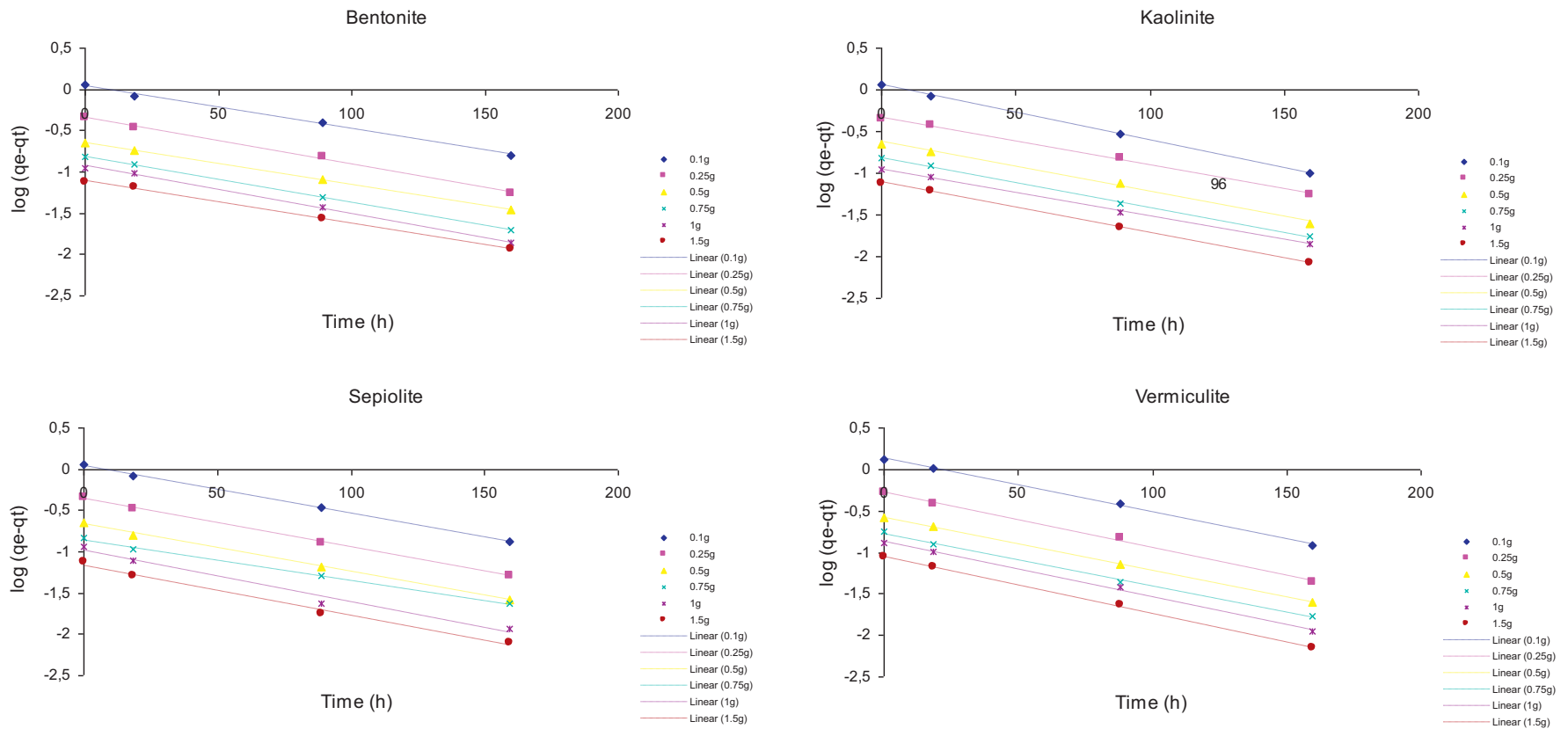
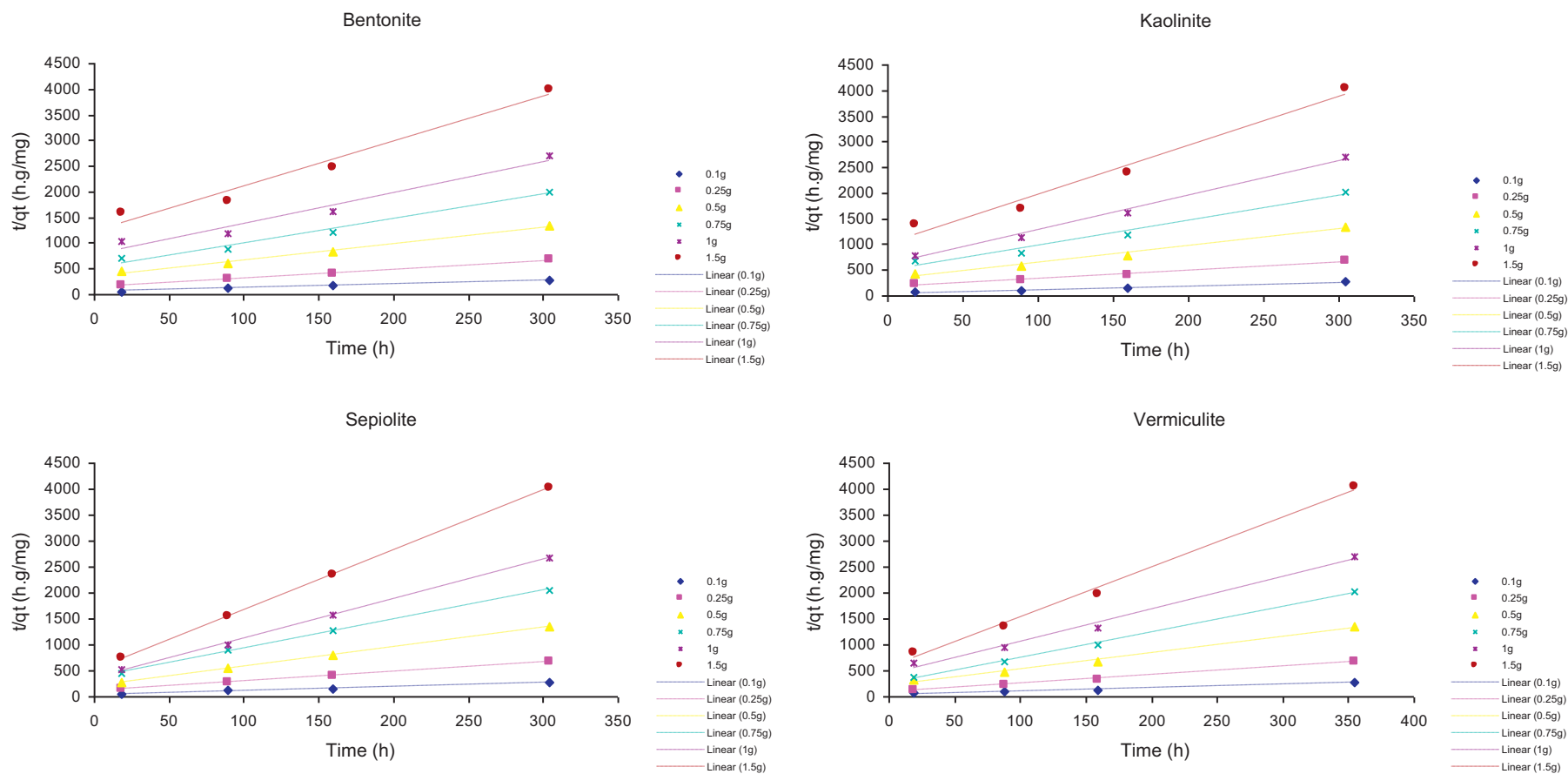


Fig. 5. Plot of pseudo-first-order kinetics for the adsorption of solvent onto different clays for an initial concentration of solvent of 800 mg/L (in 150 mL) and adsorbent doses between 0.1 g and 1.5 g.



**Fig. 6.** Plot of pseudo-second-order kinetics for the adsorption of solvent onto different clays for an initial concentration of solvent of 800 mg/L (in 150 mL) and adsorbent doses between 0.1 g and 1.5 g.

**Table 2**

Comparison of the pseudo-first-order and pseudo-second-order kinetic models for the adsorption of solvent onto the clays at various mass of adsorbents (800 mg/L of solvent).

Bentonite								
Mass (g)	$q_e$ exp (mg/g)	Pseudo first order			Pseudo second order			
		$q_e$ cal (mg/g)	$k_1$ (h)	$R^2$	$q_e$ cal (mg/g)	$k_2$ (g/mg h)	$R^2$	
0.1	1.12	1.09	0.0052	0.9972	1.38	0.0101	0.9980	
0.25	0.45	0.46	0.0057	0.9972	0.58	0.0211	0.9976	
0.5	0.23	0.23	0.0051	1.0000	0.31	0.0290	0.9935	
0.75	0.15	0.15	0.0056	0.9995	0.21	0.0423	0.9824	
1	0.11	0.12	0.0058	0.9985	0.17	0.0474	0.9614	
1.5	0.08	0.08	0.0051	0.9993	0.11	0.0620	0.9680	
Kaolinite								
Mass (g)	$q_e$ exp (mg/g)	Pseudo first order			Pseudo second order			
		$q_e$ cal (mg/g)	$k_1$ (h)	$R^2$	$q_e$ cal (mg/g)	$k_2$ (g/mg h)	$R^2$	
0.1	1.14	1.13	0.0066	0.9999	1.40	0.0113	0.9954	
0.25	0.45	0.47	0.0058	0.9980	0.63	0.0150	0.9857	
0.5	0.23	0.24	0.0060	0.9957	0.31	0.0318	0.9869	
0.75	0.15	0.15	0.0060	0.9992	0.21	0.0488	0.9780	
1	0.11	0.11	0.0056	0.9993	0.15	0.0778	0.9931	
1.5	0.08	0.08	0.0060	0.9994	0.10	0.0906	0.9743	
Sepiolite								
Mass (g)	$q_e$ exp (mg/g)	Pseudo first order			Pseudo second order			
		$q_e$ cal (mg/g)	$k_1$ (h)	$R^2$	$q_e$ cal (mg/g)	$k_2$ (g/mg h)	$R^2$	
0.1	1.17	1.10	0.0057	0.9992	1.38	0.0109	0.9994	
0.25	0.45	0.44	0.0059	0.9991	0.55	0.0296	0.9995	
0.5	0.23	0.21	0.0057	0.9980	0.27	0.0644	0.9998	
0.75	0.15	0.14	0.0049	0.9958	0.18	0.0831	0.9975	
1	0.11	0.10	0.0063	0.9834	0.13	0.1667	0.9991	
1.5	0.08	0.07	0.0061	0.9910	0.09	0.2548	1.000	
Vermiculite								
Mass (g)	$q_e$ exp (mg/g)	Pseudo first order			Pseudo second order			
		$q_e$ cal (mg/g)	$k_1$ (h)	$R^2$	$q_e$ cal (mg/g)	$k_2$ (g/mg h)	$R^2$	
0.1	1.31	1.36	0.0065	0.9983	1.63	0.0080	0.9868	
0.25	0.52	0.53	0.0067	0.9964	0.62	0.0279	0.9961	
0.5	0.26	0.27	0.0065	0.9998	0.32	0.0430	0.9883	
0.75	0.18	0.17	0.0063	0.9978	0.20	0.0935	0.9978	
1	0.13	0.14	0.0067	0.9966	0.16	0.0886	0.9906	
1.5	0.09	0.09	0.0069	0.9995	0.10	0.1628	0.9938	

The pseudo-first order model assumes that the interaction rate is limited by only one process or mechanism on a single class of sorbing sites and that all sites are time dependent [27]. The correlation coefficients were always greater than 0.99. The predicted equilibrium biosorption capacity values are in agreement to the experimental equilibrium uptake values (Table 2). In the case of the pseudo-second order model, the correlation coefficients were found to be around 0.98–0.99, but the calculated  $q_e$  was not equal to the experimental  $q_e$ , suggesting the insufficiency of the model to fit the kinetic data for the conditions of the assay. This evidence also showed that a good correlation coefficient is not a guarantee of a good agreement between the experimental and the calculated values.

#### 4. Conclusions

It was demonstrated that bentonite, sepiolite, kaolinite and vermiculite clays are able to remove efficiently diethylketone from aqueous solutions. The best isotherm fit for bentonite and kaolinite clays was obtained with the Sips model while the Dubinin–Raduskevich model was the best option for sepiolite and vermiculite. Almost complete removal of diethylketone was achieved for all clays, with values of removal percentages

approximately 97%. FTIR analyses showed a significant number of functional groups on the clays that could be responsible for adsorption of the diethylketone. A possible mechanism to explain the adsorption is that diethylketone molecules could replace water molecules on the surface of clays. Finally, the solvent affinity for the clays was found to be in the sequence vermiculite > bentonite = sepiolite = kaolinite. The procedures described herein may be suitable for treating solvent contaminated wastewater in general.

#### Acknowledgements

The authors gratefully acknowledge the financial support by the Fundação para a Ciência e Tecnologia, Ministério da Ciência e Tecnologia, Portugal. Hugo Figueiredo thanks FCT for a PhD grant (SFRH/28201/BD/2006) and Cristina Quintelas thanks FCT for a Post doctoral grant (SFRH/BPD/32113/2006). The authors would like also to thank to Minas de Barqueiros, S.A., Prof Rui Boaventura (FEUP-Portugal) and Prof Isabel Correia Neves (Dep. Química, UM, Portugal) who kindly supplied the clays and to Dr. A.S. Azevedo for collecting the powder diffraction data (Dep. of Earth Sciences, UM, Portugal). Russell Paterson is thanked for language editing.

## References

- [1] K. Pielech-Przybylska, K. Zieminski, J. Szopa St, Acetone biodegradation in a trickle-bed biofilter, *Int. Biodet. Biodegr.* 57 (2006) 200–206.
- [2] M.B. Osuna, J. Sipma, M.A.E. Emanuelsson, M.F. Carvalho, P.M.L. Castro, Biodegradation of 2-fluorobenzoate and dichloromethane under simultaneous and sequential alternating pollutant feeding, *Water Res.* 42 (2008) 3857–3869.
- [3] S.J. Wu, L.L. Zhang, J.D. Wang, J.M. Chen, *Bacillus circulans* WZ-12—a newly discovered aerobic dichloromethane-degrading methylotrophic bacterium, *Appl. Microbiol. Biotechnol.* 76 (2007) 1289–1296.
- [4] T.T. Tsai, C.M. Kao, T.Y. Yeh, S.H. Lianga, H.Y. Chien, Application of surfactant enhanced permanganate oxidation and biodegradation of trichloroethylene in groundwater, *J. Hazard. Mater.* 161 (2009) 111–119.
- [5] S.-M. Wang, S.-K. Tseng, Reductive dechlorination of trichloroethylene by combining autotrophic hydrogen-bacteria and zero-valent iron particles, *Bioresour. Technol.* 100 (2009) 111–117.
- [6] O. Hernandez-Ramirez, S.M. Holmes, Novel and modified materials for wastewater treatment applications, *J. Mater. Chem.* 18 (2008) 2751–2761.
- [7] K.G. Bhattacharyya, S. Sen Gupta, Influence of acid activation on adsorption of Ni(II) and Cu(II) on kaolinite and montmorillonite: kinetic and thermodynamic study, *Chem. Eng. J.* 136 (2008) 1–13.
- [8] A.A. El-Bayaa, N.A. Badawy, E.A. Alkhalik, Effect of ionic strength on the adsorption of copper and chromium ions by vermiculite pure clay mineral, *J. Hazard. Mater.* 170 (2009) 1204–1209.
- [9] S.S. Tahir, N. Rauf, Removal of a cationic dye from aqueous solutions by adsorption onto bentonite clay, *Chemosphere* 63 (2006) 1842–1848.
- [10] C. Quintelas, Z. Rocha, B. Silva, B. Fonseca, H. Figueiredo, T. Tavares, Removal of Cd(II), Cr(VI), Fe(III) and Ni(II) from aqueous solutions by an *E. coli* biofilm supported on kaolin, *Chem. Eng. J.* 149 (2009) 319–324.
- [11] S. Kocaoba, Adsorption of Cd(II), Cr(III) and Mn(II) on natural sepiolite, *Desalination* 244 (2009) 24–30.
- [12] E. Demirbas, M.Z. Nas, Batch kinetic and equilibrium studies of adsorption of Reactive Blue 21 by fly ash and sepiolite, *Desalination* 243 (2009) 8–21.
- [13] M. Chelly, A. Kriaa, N. Hamdi, E. Srasra, Evolution of PZC with thermal transformation of Tunisian kaolinite, *Surf. Eng. Appl. Electrochem.* 45 (2009) 232–238.
- [14] B. Benguella, A. Yacouta-Nour, Adsorption of bezanyl red and nylomine green from aqueous solutions by natural and acid-activated bentonite, *Desalination* 235 (2009) 276–292.
- [15] M. Doğan, Y. Turhan, M. Alkan, H. Namli, P. Turan, Ö. Demirbaş, Functionalized sepiolite for heavy metal ions adsorption, *Desalination* 230 (2008) 248–268.
- [16] G. Valdrè, D. Malferrari, D. Marchetti, M.F. Brigatti, The effect of different plasma gas environments on vermiculite layer, *Appl. Clay Sci.* 35 (2007) 76–84.
- [17] J. Lin, Q. Tang, J. Wu, H. Sun, Synthesis, characterization, and properties of polypyrrole/expanded vermiculite intercalated nanocomposite, *J. Appl. Polym. Sci.* 110 (2008) 2862–2866.
- [18] M. Alkan, Ö. Demirbas, M. Dogan, Electrokinetic properties of sepiolite suspensions in different electrolyte media, *J. Colloid Interface Sci.* 281 (2005) 240–248.
- [19] E.I. Unuabonah, G.U. Adie, L.O. Onah, O.G. Adeyemi, Multistage optimization of the adsorption of methylene blue dye onto defatted *Carica papaya* seeds, *Chem. Eng. J.* 155 (2009) 567–579.
- [20] B.H. Hameed, Evaluation of papaya seeds as a novel non-conventional low cost adsorbent for removal of methylene blue, *J. Hazard. Mater.* 162 (2009) 939–944.
- [21] R. Sips, Combined form of Langmuir and Freundlich equations, *J. Chem. Phys.* 16 (1948) 490–495.
- [22] M.M. Dubinin, L.V. Radushkevich, Equation of the characteristic curve of activated charcoal, *Chem. Zentr.* 1 (1947) 875.
- [23] K. Vijayaraghavan, Y.-S. Yun, Utilization of fermentation waste (*Corynebacterium glutamicum*) for biosorption of Reactive Black 5 from aqueous solution, *J. Hazard. Mater.* 141 (2007) 45–52.
- [24] M. Kumar, L. Philip, Adsorption and desorption characteristics of hydrophobic pesticide endosulfan in four Indian soils, *Chemosphere* 62 (2006) 1064–1077.
- [25] M. Khamis, F. Jumean, N. Abdo, Speciation and removal of chromium from aqueous solution by white, yellow and red UAE sand, *J. Hazard. Mater.* 169 (2009) 948–952.
- [26] M.A. Al-Ghouti, M.A.M. Khraisheh, M.N.M. Ahmad, S. Allen, Adsorption behaviour of methylene blue onto Jordanian diatomite: a kinetic study, *J. Hazard. Mater.* 165 (2009) 589–598.
- [27] B. Fonseca, H. Maio, C. Quintelas, A. Teixeira, T. Tavares, Retention of Cr(VI) and Pb(II) on a loamy sand soil: kinetics, equilibria and breakthrough, *Chem. Eng. J.* 152 (2009) 212–219.